

# Simulation of Ground Level Spectral Solar Irradiance in Rwanda using LibRadtran.

**MC Cyulinyana and H. Winkler**

University of Johannesburg, Physics Department, PO Box 524, 2006 Auckland Park,  
Johannesburg, South Africa

E-mail: kamirwa@gmail.com

**Abstract.** Optimizing solar power development in Rwanda requires accurate knowledge of the spectral distribution of solar irradiation reaching the Earth's surface at different wavelengths. To characterize the effect of aerosols on surface solar irradiance, the simulation of a cloudless atmosphere is presented in this study. The irradiance spectrum is obtained by solving the radiative transfer equation for this aerosol distribution using established radiative transfer codes. The results show a spectral distribution simulated using LibRadtran, which is one such software package. Its main program, UVSPEC is a radiative transfer tool mainly used to compute radiances, irradiances, and actinic fluxes in the solar and thermal spectral regions. The aerosol properties are furthermore investigated through comparison with archival sunphotometry data from the region and their effect on the surface solar radiation. It is then shown how the outcome of this calculation may be used to estimate local energy yield.

## 1. Introduction

Solar radiation at the Earth's surface varies greatly due to the change in relative position of the Sun, both during the day and over the year, but also due to the change of atmospheric conditions [1, 2]. Cloud cover, air pollution, the latitude of a location, and time of the year all cause variations in solar irradiance at the Earth's surface [3]. The following types of solar radiation in the Earth's atmosphere are typically defined: (i) direct radiation, which comes direct from the Sun without any interaction; (ii) diffuse radiation, which comes from all over the atmosphere as a result of reflection and scattering by clouds and other atmosphere particles or molecules; and (iii) global horizontal radiation, which is the sum of direct and diffuse radiation on a horizontal surface [1, 4, 5]. In order to optimize locations for solar energy platforms, a ground level spectral solar irradiance distribution is desirable.

Good solar radiation data at ground level is also essential for a wide range of applications in engineering, meteorology, agricultural sciences, in health science, and other fields of natural science to name just a few [6]. The lack of widespread solar ground measurement equipment and meteorological stations leads to insufficient knowledge of solar energy potential in many developing countries. Solar radiation data would help to find solutions to energy shortage and environmental degradation in those areas [7]. This knowledge helps decision and policy makers in energy sectors, especially for green energy technology implementation.

Even though many methods have been used to estimate and model solar radiation at ground level in the past [3, 4, 8], radiative transfer models have not been widely used, especially in a country like Rwanda where solar modelling was based on empirical and meteorological models

[7]. In this paper, the applicability of the LibRadtran computational code to model Rwanda's solar irradiance is being studied. The procedure could equally be extended to other countries.

This study determines the change of solar spectral irradiance and its relation with aerosols over a typical tropical area (Rwanda). A case study is made of three particular days (see table 1) representing various seasons in the country, using a standard or well-established radiative transfer code [10]. The results show a spectral distribution simulated using LibRadtran, which is a software package for radiative transfer calculations [9, 10].

## 2. Modelling the Interaction of the Solar Spectrum With the Atmosphere

### 2.1. Radiative Transfer Equation

The interaction of electromagnetic radiation as it propagates through a medium, is described by the radiative transfer equation (RTE). RTE is widely used to describe and understand the atmospheric radiative transfer of solar radiation [1, 5, 11]. As solar radiation at location  $(x, y, z)$  propagates through the atmosphere, it experiences absorption, emission, and scattering [9, 11].

To solve the RTE is non-trivial. It is usually not possible to obtain the solution in a simple analytical function. A common approach is to apply numerical computational methods to solve the RTE and compute the solar irradiance under specific circumstances [10]. The RTE gives the radiance field when solved with appropriate boundary conditions [3]. The solution of the RTE generally yields the diffuse irradiance and the direct irradiance, which in turn are added to give total irradiances or flux quantities [9, 10].

### 2.2. The Downward Spectral Irradiance

The downward spectral irradiance (the electromagnetic power per unit area received from the Sun radiation in a given wavelength range)  $I_{\lambda\downarrow}$  is given by the sum of two components: the spectral direct  $I_{\lambda\text{dir}}$  and spectral diffuse  $I_{\lambda\text{diff}}$  irradiance.

$$I_{\lambda\downarrow} = I_{\lambda\text{dir}} + I_{\lambda\text{diff}} \quad (1)$$

Equation (1) can be rewritten in terms of direct transmittance (light fraction passing through the atmosphere without being attenuated)  $T_{\lambda\text{dir}\downarrow}$  and diffuse transmittance (transmitted light fraction after being scattered/attenuated)  $T_{\lambda\text{diff}\downarrow}$  and becomes:

$$I_{\lambda\downarrow} = I_{E\lambda}\mu_0 (T_{\lambda\text{dir}\downarrow} + T_{\lambda\text{diff}\downarrow}), \quad (2)$$

where  $I_{E\lambda}$  represents the extraterrestrial normal irradiance at an average wavelength  $\lambda$  and  $\mu_0$  is the cosine of solar incident angle ( $\theta_z$ ) (an angle that light ray makes with the normal to the surface at the point where the ray meets the surface). We use the approximation of a plane parallel atmosphere divided into two non-mixing layers. One consists of molecules modelled with Rayleigh scattering [12, 13], whose Rayleigh optical depth (the measure of molecules distributed within a column of air from the Earth's surface to the top of the atmosphere)  $\tau_{r\lambda}$  and phase function  $Re(\gamma)$  are given by the following equations, respectively:

$$\tau_{r\lambda} = 0.008735\lambda^{-4.08} \frac{P_s}{P_0}, \quad (3)$$

$$Re(\gamma) = \frac{3}{4} (1 + \cos^2(\gamma)). \quad (4)$$

where  $P_s$  and  $P_0$  are site pressure and standard atmospheric pressure respectively and  $\gamma$  is the scattering angle.

The other layer is composed of aerosols. In order to model aerosols, the aerosol optical depth (AOD)  $\tau_{a\lambda}$  and scattering phase function (Henyey-Greenstein) [13] are defined as follows:

$$\tau_{a\lambda} = \beta\lambda^{-\alpha} \simeq \beta\lambda^{-1.3} \quad (5)$$

$$HG(\gamma) = \frac{1 - g^2}{(1 + g^2 - 2g \cos(\gamma))^{3/2}}, \quad (6)$$

where  $\beta$  is the Angstrom turbidity coefficient,  $\alpha$  is the Angstrom wavelength exponent, and  $\lambda$  is the wavelength in  $\mu\text{m}$ .  $\beta$  is related to the amount of aerosols present in the atmosphere, while  $\alpha$  is proportional to the size distribution of aerosols [14].  $g$  is the asymmetry parameter which describes the scattering angle distribution, and  $\gamma$  is the scattering angle. The combination of those two components gives us the total optical depth,  $\tau_\lambda$  for the modelled atmosphere.

$$\tau_\lambda = \tau_{r\lambda} + \tau_{a\lambda}. \quad (7)$$

From equation (7), the total transmittance can be expressed in term of optical depth for each layer of this modelled atmosphere and is given by  $T_{\text{tot}} = T_r T_a$ . Where  $T_a$  and  $T_r$  refer to the total transmittance through the aerosol layer and molecule layer respectively.

Considering all those parameters, the downward solar irradiance expressed in equation (2) becomes

$$I_{\lambda\downarrow} = I_{E\lambda}\mu_0 T_{\text{tot}} \quad (8)$$

### 2.3. Model Description of Irradiance

Radiative transfer models (RTMs) use information about the optical properties of the Earth's atmosphere such as single scattering albedo ( $\omega_0$ ), aerosol optical depth ( $\tau_{a\lambda}$ ), asymmetry parameter ( $g$ ), aerosol models and different atmospheric profiles as input to determine a theoretical solar irradiance at the Earth's surface [5, 11]. To determine the degree to which incoming solar light is affected by aerosols we used libRadtran to simulate spectral irradiance. LibRadtran is a library of radiative transfer routines and programs that includes a selection of twelve different radiative equation solvers, of which DISORT is most widely used. Its main function is the uvspec program which calculates the radiation field in the Earth's atmosphere [9, 15], which in turns determines irradiance, radiance, and actinic fluxes (the quantity of light available to molecules at a particular point in the atmosphere and which, on absorption, drives photochemical processes in the atmosphere)[1]. The inputs to the model are the constituents of the atmosphere including various molecules, aerosols, and clouds [10]. A tropical atmosphere profile and DISORT solver are used to evaluate the aerosol optical depth at a short wavelength range which is in visible - near infrared (VIS-NIR) region.

DISORT is based on discrete ordinates and allows users to compute irradiance in a plane-parallel geometry [10]. The AOD at several wavelengths of the solar spectrum (380, 440, 500, 675, 870 and 1020nm) and the Angstrom exponent at 440/870nm are retrieved from regional sunphotometry data [14].

By solving the RTE, a number of radiative quantities are simulated: the downward direct normal irradiance (DNI) and diffuse irradiance (DI) and the global horizontal irradiance (GHI). The irradiance is obtained by integrating the radiances, which is the radiative solar power per unit solid angle in a particular direction, weighted with the cosine of the viewing zenith angle over all viewing directions in the hemisphere ( $2\pi$  steradians) [9].

## 3. Results and Discussion

In this study, we estimate aerosols optical characteristics representing three typical atmospheric profiles in Rwanda. We did this by inspecting data from the nearest AERONET station

to Rwanda, which is in Bujumbura, Burundi (Latitude: 3.0°S and Longitude: 29.8°E), for which we assume the same atmospheric and weather profile as Rwanda (Latitude: 2.0°S and Longitude: 30.0°E). Table 1 shows the typical aerosol optical depth characterizing three

**Table 1.** Assumed AOD at 6 different wavelengths for Rwanda based on actual data retrieved from sunphotometry at Bujumbura.

Angstrom parameters ( $\alpha, \beta$ )	$\tau_{1020\text{nm}}$	$\tau_{870\text{nm}}$	$\tau_{675\text{nm}}$	$\tau_{500\text{nm}}$	$\tau_{440\text{nm}}$	$\tau_{380\text{nm}}$	$\tau_{340\text{nm}}$
Low turbidity $\alpha = 2.0, \beta = 0.03$	0.03	0.04	0.07	0.12	0.15	0.20	0.25
Moderate turbidity $\alpha = 1.5, \beta = 0.16$	0.16	0.20	0.30	0.48	0.58	0.72	0.85
High turbidity $\alpha = 1.2, \beta = 0.44$	0.46	0.56	0.76	1.1	1.28	1.52	1.72

atmospheric scenarios in Rwanda. The data show the wavelengths dependence of AOD and characterizes certain conditions under study, for a site of altitude 1490m above sea level (corresponding to Kigali international airport). To test the sensitivity of solar irradiance change in AOD, the wavelength (500nm) was used to investigate three scenarios; low turbidity ( $\tau_{500\text{nm}} = 0.12$ , April/May 2014, rainy period in Rwanda), moderate turbidity ( $\tau_{500\text{nm}} = 0.48$ , October/November is a shorter rainy season) and high turbidity ( $\tau_{500\text{nm}} = 1.1$ , July/August, dry season in Rwanda). The simulation at two different solar positions (i.e., air mass (AM)) is also presented; AM=1.5 and AM=5 which represent roughly daytime and just before sunset respectively. To calculate AOD, we adopt typical values of the wavelength exponent  $\alpha$  retrieved from AERONET data.  $\tau_{a\lambda}$  was calculated using equations (5) and (9) [14]. In this study,  $\tau_{a1\lambda_1} = \tau_{500}$  and  $\lambda_1 = 500\text{nm}$ .

$$\alpha = -\frac{\ln \frac{\tau_{a2\lambda_2}}{\tau_{a1\lambda_1}}}{\ln \frac{\lambda_2}{\lambda_1}}. \quad (9)$$

Under cloudless conditions, aerosols are the main atmospheric constituents responsible for the attenuation of solar radiation. The combination of aerosol scattering and atmospheric gas absorption are key players in the visible-near infrared (VIS-NIR) region.  $\beta$  values of less than 0.1 are associated with a relatively clear atmosphere, and values greater than 0.2 are associated with a relatively hazy atmosphere. The results show that AOD has a high impact on direct normal irradiance and the high attenuation is in the visible region (Figure 1, right). This effect has large uncertainties associated with aerosols characterization, aerosols properties (i.e. AOD,  $\omega_0$  and  $g$ ) and their horizontal and vertical profiles.

### 3.1. Effect of AOD on Spectral Irradiance Components

We used a radiative transfer model to compute spectral irradiance for a cloudless sky. A remarkable reduction in total irradiance and the increase in diffuse light depending on aerosol particles distribution has been observed (Figure 1, left and middle).

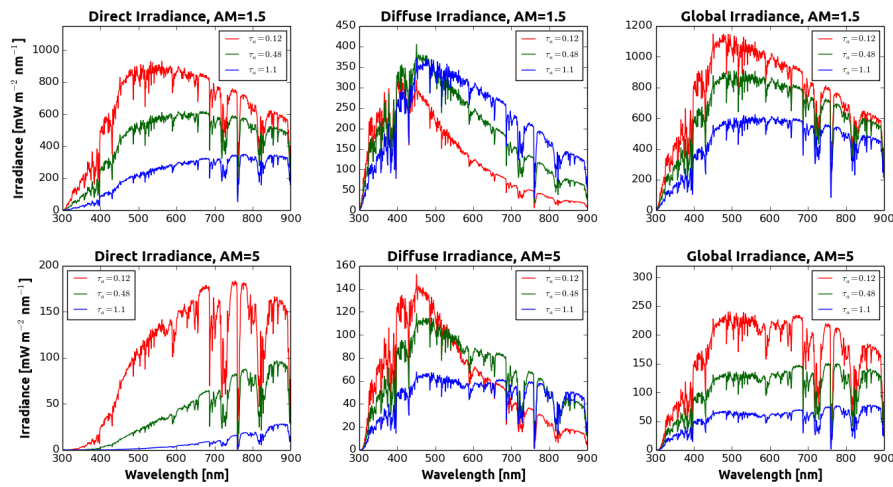


**Figure 1.** Spectral irradiance for a cloudless sky, AOD= 0.12, 0.48, 1.1. Top row represents an air mass (AM) of 1.5 used for characteristics of day time. The bottom row, represents an air mass (AM) of 5 (near sunset). Left, middle and right diagrams represent direct, diffuse and global surface irradiance.

In fact, when particle size to scatter wavelength is small, i.e. air molecules scattering visible wavelength (380-780nm), scattering is in Rayleigh regime in which short wavelengths (blues) are scattered more efficiently than long wavelengths (reds), giving the sky its blue color [3, 14]. When particles are similar in size to the scattered wavelength, scattering is more uniform across the visible spectrum. Thus, in the presence of an aerosol layer, diffuse irradiance at longer wavelengths (reds) increases more than the increase in shorter wavelengths (blues) [3, 14]. As scattering increases, the portion of diffuse light also increases, resulting in a brighter sky. Figure 1 gives more details for each solar irradiance component. The reduction of surface solar irradiance in the dry season is due to different human activities such as biomass burning while farmers are preparing for seeding season, charcoal preparation which is done by burning trees and the people movements from one place to another increase in such time, which are done by means of transport (i.e. vehicles). Those activities reproduce more atmospheric pollutants and dust particles to name few. These particles size grow due to water vapor presence in the atmosphere.

### 3.2. Effect of aerosols on Daily Solar Irradiance

Figure 2 shows the variation of surface solar irradiance on different days represented by different atmospheric conditions at 550 nm (visible light). The simulation was done from noon time when the Sun is overhead (SZA  $\approx 0^\circ$  till the sunset time (SZA  $\approx 85^\circ$ ) in a dry/rainy seasons. For example in figure 2, on a clear day when the Sun is overhead surface solar irradiance (global) is around  $1200 \text{ Wm}^{-2}\text{nm}^{-1}$  at and on a turbid day (figure 2 (bottom row)) it is slightly above  $800 \text{ Wm}^{-2}\text{nm}^{-1}$ , showing the effect on aerosol presence as expected. As the Sun changes position there is a remarkable reduction due to losses related to the optical path [3]. The increase in diffuse radiation and decrease in DNI are also observed and are represented in figure 2 (top row). The simulation results agree well with the actual recorded results. For example on a turbid day, when the Sun is overhead at Kigali international airport (3<sup>rd</sup> August 2014), surface solar irradiance varies between  $875\text{-}980 \text{ Wm}^{-2}$  which is in the same range with this study.

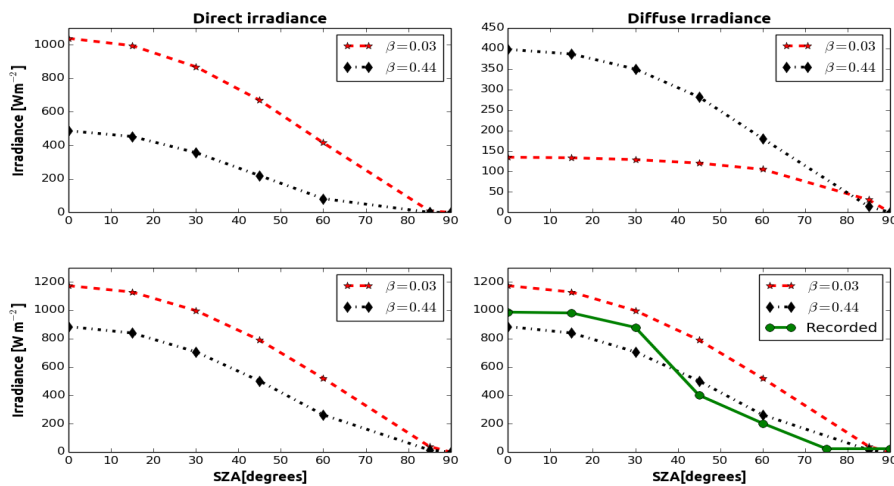


**Figure 2.** Diurnal effect of aerosol on surface irradiance at different days at  $\lambda = 550\text{nm}$ . The top row represents the variation of direct irradiance and diffuse irradiance on a clear day ( $\beta = 0.03$ ) and on turbid day ( $\beta = 0.44$ ) respectively. The bottom row represents the global irradiance variation on clear day and turbid day respectively and its comparison with recorded data

#### 4. Conclusions

The present study reports the variation of solar spectral irradiance and its relation with aerosols over a turbid tropical region (specifically Rwanda). Considerable reduction in the VIS-NIR irradiances has been projected during the period of high aerosol loading. Our simulations show that aerosols substantially decrease downward shortwave irradiances at the surface, which then impacts solar energy availability on the Earth. High  $\beta$  and  $\alpha$  values estimated on a turbid day are representative of urban environments which are similar to some reported previous studies.

This approximation of solar spectral irradiance distribution enables solar systems planners to develop more accurate technologies to estimate energy yield of photovoltaic panels and concentrated solar power plants.

#### Acknowledgements

Special thanks to Dr. Claudia Emde, for her useful assistance and discussion in developing this paper. This Ph.D. project is supported by University of Johannesburg, OWSD, and Sida.

#### References

- [1] Liou K.N., 2002, *An introduction to atmospheric radiation*, vol.84 , Academic press.
- [2] Gueymard C., 1993, *Solar Energy*, **51**, 121-138
- [3] Muneer T., 2004, *Solar Radiation and Daylight Models*, Elsevier Butterworth.
- [4] Benson R.B., et al., 1984, *Solar Energy*, **32**, 523-535
- [5] Iqbal M., 2012, *An introduction to solar radiation*, Elsevier.
- [6] Gueymard C., 2004, *Solar Energy*, **76** 423-454
- [7] Safari B., Gasore J., 2009, *Asian Journal of Scientific Research*, **2**, 68-75
- [8] Mi Zhou H., et al., 2005, *J.Geophys.Res*, **110**, 1-10
- [9] Mayer B., 2009, *Eur.Phys.J.Conferences*, **1**, 75-99
- [10] Emde C., et al., 2016, *Geosci. Model Dev*, **9**, 1647-1672
- [11] Buglia J., 1986, NASA-RP-1156, L16068, NAS 1.61:1156
- [12] Bucholtz A., 1995, *J.Ap.Opt*, **34** 2765-2773
- [13] Prahl S., et al., 1989, *J. Dos. of. Las. Rad. in Med. and Bio.*, **5** 102-111
- [14] Dubovik O., at al., 2002, *J.Atm.Sc*, **59**, 590-608
- [15] Lorente J., et al., 1994, *J.Ap.Meteo*, **33**, 406-415